WPMAG-CPR(17) 18606

A Dembkowska et al.

# Helium Flow and Temperature Distribution in the CS1 module of the DEMO CS coil

Preprint of Paper to be submitted for publication in Proceeding of 9th International Conference Electromagnetic Devices and Processes in Environment Protection ELMECO-9 with 12th Seminar

This work has been carried out within the framework of the EUROfusion Consortium and has received funding from the Euratom research and training programme 2014-2018 under grant agreement No 633053. The views and opinions expressed herein do not necessarily reflect those of the European Commission.

# Helium Flow and Temperature Distribution in the CS1 module of the DEMO CS coil

Aleksandra Dembkowska, Monika Lewandowska
Faculty of Mechanical Engineering and Mechatronics
West Pomeranian University of Technology
Szczecin, Poland
monika.lewandowska@zut.edu.pl

Xabier Sarasola
Swiss Plasma Center (SPC)
École Polytechnique Fédérale de Lausanne (EPFL)
Villigen, Switzerland

***Abstract*—Two alternative designs of the CS1 module for the DEMO Central Solenoid (CS) coil have recently been proposed by EPFL-SPC PSI Villigen and CEA Cadarache. According to the SPC design the CS1 module consists of 10 sub-coils, each of which includes 2 layers wound using the same kind of conductor. The two innermost sub-coils utilize Re-123 High $T_c$ Superconductor (HTS), the next five sub-coils are made of R&W $Nb_3Sn$ conductors, and the three most outer sub-coils use NbTi. In the present work we study thermal-hydraulic phenomena which may occur in the CS1 coil (SPC design) at the normal operating conditions. Time evolution of the mass flow rate, temperature, pressure and $T_{cs}$ profiles in each conductor during the whole current cycle are simulated using the THEA code from Cryosoft. We take into account time evolution of the magnetic field and AC losses heat load profiles in each conductor.**

**Keywords—DEMO, Central Solenoid (CS) coil, CS1 module, thermal – hydraulic analysis, low temperature superconductor, high temperature superconductor**

## I. INTRODUCTION

The European DEMO tokamak will be the next generation fusion demonstration reactor that will follow ITER project. The main purpose of conceptual studies of DEMO, performed under the lead of the EUROfusion Consortium [1]-[3], is to demonstrate feasibility of grid electricity production at the level of several hundred MW. Fusion reactor magnet system is one of the most demanding parts of a tokamak in terms of conceptual studies, i.e. it requires complete mechanical, electromagnetic, and thermal-hydraulic analyses at normal operating conditions, as well as during quench that may occur in superconducting coils. The superconducting magnet system of the DEMO fusion reactor will consist of following elements: toroidal field (TF) coils, poloidal field (PF) coils and central solenoid (CS).

In 2015 two alternative designs of the CS coil for the European DEMO fusion reactor were proposed by EPFL-SPC PSI Villigen and CEA Cadarache [4]-[6]. The DEMO CS coil will be divided into five modules, i.e. CSU3, CSU2, CS1, CSL2 and CSL3, according to the 2015 DEMO reference [7]. This paper is aimed at study thermal – hydraulic phenomena which may occur in the CS1 module (SPC design), subjected to the highest magnetic fields and mechanical loads from all DEMO CS modules. Time evolution of the mass flow rate, temperature, pressure and current sharing temperature ($T_{cs}$) profiles at normal operating conditions in each conductor during the whole current cycle are investigated using the THEA code from Cryosoft [8]-[9].

## II. Conductors' Characteristics

The preliminary design of CS1 winding pack was presented in [4]. Here we study the 3rd iteration of the design, the most mature of those presented in detail in [5]. The CS1 is a graded layer wound coil, consisting of 10 sub-coils (SC). Each SC has 2 layers made of the same conductor grade. The two innermost SC, located in the highest magnetic field, are made of RE-123 High $T_c$ Superconductor (HTS). The rest of SC is wound with Low $T_c$ Superconductor (LTS) cables. The 3rd – 7th SC, placed in medium magnetic field, utilize R&W $Nb_3Sn$ conductors, whereas the 8th – 10th SC, subjected to low magnetic field, are made of NbTi conductors. The LTS conductors are flat multistage cables with two side and one rectangular helium cooling channels (Fig. 1a). Those elements are encased in solid Cu/CuNi stabilizer. The whole construction is enclosed in a steel jacket.

The HTS conductor (Fig. 1b) is a flat cable with strands made of twisted stack of HTS tapes soldered into a copper profile. Strands are arranged around a copper core and surrounded by a stainless steel conduit. Conductors parameters used in the present analysis were described in detail in [5] and [10]. It is assumed that the superconductors' properties are based on the scaling laws presented in [4].

## III. Model Assumptions

THEA model of each LTS conductor consists of several
1-D parallel components – three thermal components (strands, stabilizer and steel jacket) and three hydraulic components (He in the bundle, He in the side channels, He in the upper rectangular channel).


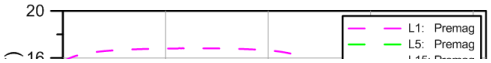


The boundary between the steel jacket and the stabilizer is not tight, thus helium can flow between the side and rectangular cooling channels. The helium exchange between all cooling channels and the bundle region is also allowed. The HTS conductor also consists of three thermal components, i.e. copper core, strands and a steel conduit, but it has only one hydraulic component, namely He in a cable space. The heat-exchange links between individual cable components were assumed according to the THEA model presented in [10]. As in previous studies of DEMO TF coil [11]-[15], for describing flow in the LTS bundle region, the friction factor correlation based on the porous medium Darcy – Forchheimer equation [16] is utilized, whereas for all the cooling channels the smooth tube Bhatti - Shah correlation [17] is used. According to [18], for the flow in HTS cable space, we assume the Fanning friction factor correlation developed for the EURATOM LCT conductor [19]. The heat transfer between adjacent turns was also taken into account.

We assume that the CS coil is cooled by helium
the cc
equals
Assum
are si
therm
[11]-[1

Fig. 1. Schematic layout of a (a) HTS, (b) LTS cable.

The
conductor in each SC (subjected to the higher magnetic field), was simulated during whole current cycle. We assume the following reference current scenario: 10 s premagnetisation phase (Premag), 80 s plasma current ramp-up (PCRU) phase, 2 hour burn phase (between the Start of Flat Top (SOF) and the End of Flat Top (EOF)) and 10 min dwell phase (between EOF and beginning of Premag). In the Premag phase, the operating current is constant and has the maximum value, $I_{Premag}$ = 51.22 kA [5]. We also assumed the ratio of operating current: $I_{Premag}$ : $I_{SOF}$ : $I_{EOF}$ = 57.14 : -8.79 : -57.14 [22]. Operating current during the

This work was carried out within the framework of the EUROfusion Consortium and was supported in part by the Euratom Research and Training Program 2014–2018 under Grant 633053 and in part by the Polish Ministry of Science and Higher Education within the framework of the financial resources in the year 2017 allocated for the realization of the international cofinanced project. The views and opinions expressed herein do not necessarily reflect those of the European Commission.

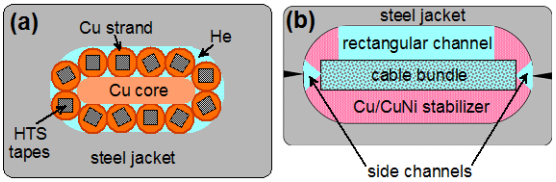


Fig. 1. Schematic layout of a (a) HTS, (b) LTS cable.

PCRU, burn and dwell phases was obtained by linear interpolation of current values in characteristic points: Premag, SOF and EOF.

The realistic magnetic field distribution $B(x,t)$ and the heat load due to AC coupling losses $P_{coupling}(x,t)$ were calculated according to the methodology developed in [10]. The magnetic field profiles at the premagnetisation phase, as well as at the characteristic points of the current cycle, namely SOF and EOF, is shown in Fig. 2. We present examples of the magnetic field distribution in layers L1, L5 and L15, i.e. in the shorter conductor of the 1st SC (HTS), 3rd SC ($Nb_3Sn$) and 8th SC (NbTi), respectively.

According to [20], the AC coupling losses were calculated using the formula:

$$P_{coupling}(x) = \frac{n\tau S}{\mu_0}\left(\frac{d\vec{B}(x)}{dt}\right)^2 = \frac{n\tau S}{\mu_0}\left[\left(\frac{dB_r(x)}{dt}\right)^2 + \left(\frac{dB_z}{d}\right.\right. \quad (1)$$

where $n$ is the shape factor, $\tau$ is a time constant dependent on the conductor parameters, $S$ is the conductor cross section (excluding helium and jacket) and $x$ is the coordinate along the conductor. As agreed with the project team, the assumed $n \cdot \tau$ value for calculating AC coupling losses in the DEMO CS conductors, is equal to 75 ms [21], which is the target value for the conductors' designers. The examples of calculated $P_{coupling}$ profiles in the PCRU, burn and dwell phases in layers L1, L5 and L15 are presented in Fig. 3. It is worth to notice, that in the premagnetisation phase AC coupling losses equals zero since the magnetic field profiles in each layer are constant during the Premag phase. The AC losses in each layer in the PCRU phase are typically several thousand times larger than in the burn phase and dozen times larger than in the dwell phase.

## IV. Results and Discussion

As the initial stage of our study, we performed the preliminary THEA simulations of conductors' operation during the premagnetisation phase assuming no heat load, constant magnetic field profiles along the conductors (see examples in Fig. 2) and setting current to constant value of 51.22 kA. As the initial conditions we assumed $T(x) = 4.5$ K and $p(x) = 0.6$ MPa. These simulations lasted till the stationary state was achieved. Then the obtained steady states temperature, pressure, mass flow rates profiles in each conductor were used as the initial conditions for the consecutive whole current cycle simulations.

Some typical examples of the time evolution of temperature profiles for analyzed HTS (L1), $Nb_3Sn$ (L5) and NbTi (L15) conductors, starting from the end of the premagnetisation phase ($t$ = 10 s) till the end of the PCRU phase ($t$ = 90 s) are presented in Fig. 4. The temperature profiles in the last seconds of the dwell phase were also added. During the PCRU phase the temperature rises fast due to relatively large AC losses (see Fig. 3), but also the simultaneous rise of the current sharing temperature can be observed (see Fig. 5), as an effect of declining both magnetic field (see Fig. 2) and operating current. The $T_{cs}$ rise is much larger than the increase in temperature, therefore the temperature margin, defined as a difference between these two values, grows in subsequent seconds of the PCRU phase. The current sharing temperature in the very last second of the dwell phase is similar to the low $T_{cs}$ value during the premagnetisation phase, but in contrast to this phase the AC coupling losses during the dwell phase are not equal to 0 W/m, which results in higher temperature profiles in 7888 s of the current cycle. Therefore, the minimum value of temperature margin appears in the very last seconds of current cycle,

despite the fact that during the dwell phase $P_{coupling}$ are significantly lower than in the PCRU phase (see Fig. 3).

In temperature profiles of the analyzed HTS conductors a characteristic temperature peak is observed. The peak arises in the first 2 seconds of the PCRU phase ($t$ = 12 s) at the left boundary of the conductor, and in the further course of the PCRU phase it propagates towards the middle of the cable (see fig. 4a). This effect is accompanied by the pressure increase above the inlet pressure (0.6 MPa). The maximum pressure value and the maximum of the temperature peak are observed in the same location (see Figs. 4a and 6a), further referred to as "$X_{peak}$". As a consequence, the helium flow reversal is observed in the left part of a cable, i.e. for $X < X_{peak}$, whereas in the right part of a cable ($X > X_{peak}$) helium flow

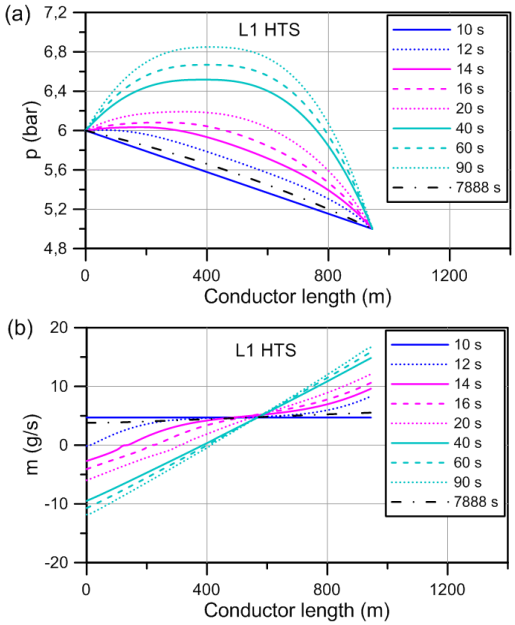


Fig. 6. Time evolution of the (a) pressure profile and (b) mass low rate profile in the first (HTS) layer of winding pack.

is accelerated (see Fig. 6b). In the 2nd SC the qualitative results were similar, but the quantitative increase in temperature was lower, so a weaker pressure rise above 0.6 MPa and the weaker backflow effect was observed. These phenomena occur only during the PCRU phase, because the $P_{coupling}$ values during the dwell and the burn phases are insufficient to induce the formation of the temperature peak and the flow reversal (see Figs. 7a, 7b). During the PCRU phase, slowing down of helium in the left half of $Nb_3Sn$ conductors and accelerating in the right half, is observed, but the backflow effect does not occur (Fig. 7a).

## V. Summary and Conclusions

The thermal – hydraulic behavior of the CS1 module at normal operation was simulated using the THEA code during the whole plasma scenario (the PCRU, burn and dwell phases). Realistic distribution of the magnetic field, heat load caused by AC coupling losses, inter-turn heat transfer and mass transfer between all channels of flow were taken into account.

Time evolution of the mass flow rate, temperature, pressure and $T_{cs}$ profiles in the inner conductor of each sub-coil were calculated. According to the performed analysis, the minimum value of temperature margin in each conductor appears in the very last seconds of the current cycle. In HTS conductors, the helium backward flow was observed during the PCRU phase. The backflow was accompanied by pressure increase above the inlet pressure and characteristic temperature peak. In LTS conductors, these effects did not appear.

## *References*


[1] "Fusion Electricity. A roadmap to the realisation of fusion energy," November 2012, Available: https://www.euro-fusion.org/wpcms/wp-content/uploads/2013/01/JG12.356-web.pdf

[2] G. Federici, *et al*., "Overview of the design approach and prioritization of R&D activities towards an EU DEMO," Fusion Eng. Des., vol. 109–111, pp. 1464–1474, November 2016.

[3] G. Federici, *et al.*, "DEMO Design Activity in Europe: Progress and Updates," Fusion Eng. Des., in press.

[4] R. Wesche, N. Bykovsky, X. Sarasola, K. Sedlak, B. Stepanov, D. Uglietti, and P. Bruzzone, "Central solenoid winding pack design for DEMO," Fusion Eng. Des., submitted in Fusion Eng. Des., unpublish.

[5] R. Wesche and X. Sarasola, "Report on CS Winding Pack Design and Analysis," Final report MAG-2.1-T004-D003, 2017, https://idm.euro-fusion.org/?uid=2MRPVA

[6] R. Vallcorba, B. Lacroix, D. Ciazynski, A. Torre, F. Nunio, L. Zani, Q. Le Coz, S. Nicollet, V. Corato, and M. Coleman, "Thermohydraulic Analyses on CEA Concept of TF and CS Coils for EU-DEMO,", submitted in IEEE Trans. Appl. Supercond., unpublished.

[7] B. Meszaros, "EU DEMO1 2015 – DEMO-Tokamak-Complex," (CAD Model), 2015, https://idm.euro-fusion.org/?uid=2D3FBF .

[8] L. Bottura, C. Rosso, and M. Breschi, "A general model for thermal, hydraulic and electric analysis of superconducting cables," Cryogenics, vol. 40, no. 8–10, pp. 617–626, Aug.–Oct. 2000.

[9] THEA—Thermal, Hydraulic and Electric Analysis of Superconducting Cables. User's Guide Version 2.3, CryoSoft, Sept. 2016, Available: https://supermagnet.sourceforge.io/manuals/Thea_2.3.pdf .

[10] A. Dembkowska, M. Lewandowska and X. Sarasola, "Thermal-Hydraulic Analysis of the DEMO CS coil", submitted in IEEE Trans. Appl. Supercond., unpublished.

[11] M. Lewandowska and K. Sedlak, "Thermal-hydraulic analysis of LTS cables for the DEMO TF coil," IEEE Trans. Appl. Supercond., vol. 24, no. 3, Art. no. 4200305, June 2014.

[12] M. Lewandowska, K. Sedlak and L. Zani, "Thermal-hydraulic analysis of the low-$T_c$ Superconductor (LTS) winding pack design concepts for the DEMO Toroidal Field (TF) coil," IEEE Trans. Appl. Supercond., vol. 26, no. 4, Art. no. 4205305, June 2016.

[13] R. Zanino et al., "Development of a Thermal-Hydraulic Model for the European DEMO TF Coil," IEEE Trans. Appl. Supercond., vol. 26, no. 4, Art. no. 4201606, June 2016.

[14] R. Vallcorba et al., "Thermo-hydraulic analyses associated with a CEA design proposal for a DEMO TF conductor," Cryogenics, vol. 80, pp. 317–324, December 2016,

[15] K. Sedlak, P. Bruzzone and M. Lewandowska, "Thermal-hydraulic and quench analysis of the DEMO toroidal field winding pack WP1," Fus. Eng. Des., in press.

[16] M. Bagnasco, L. Bottura, and M. Lewandowska, "Friction factor correlation for CICC's based on a porous media analogy," Cryogenics, vol. 50, no. 11/12, pp. 711–719, Nov.-Dec. 2010

[17] R.K. Shah, D.P. Sekulić, "Fundamentals of Heat Exchanger Design", Wiley, New Jersey, 2003, pp. 482.

[18] R. Heller, P. V. Gade, W.H. Fietz, Senior M, T. Vogel, and K.-P.Weiss, "Conceptual Design Improvement of a Toroidal Field Coil for EU DEMO Using High-Temperature Superconductors," IEEE Trans. Appl. Supercond., vol. 26, no. 4, Art. no. 4201105, June 2016,

[19] D. S. Beard, W. Klose, S. Shimamoto, and G. Vecsey, "The IEA largecoil task development of superconducting toroidal field magnets for fusion power," Fusion Eng. Des., vol. 7, no. 1/2, pp. 1–230, 1988.

[20] A.M. Campbell, "A general treatment of losses in multifilamentary superconductors," Cryogenics, vol. 22, no. 1, pp. 3–16, January 1982.

[21] ITER Design Description Document. Magnets. Section 7: Conductors, ITER_D_2NBKXY v1.2, 2009.